

## Investigation on the crystallization behaviour of sodium-aluminoborosilicate glasses with high concentrations of Ba and Ti

R. Harizanova<sup>1\*</sup>, D. Tatchev<sup>2</sup>, G. Avdeev<sup>2</sup>, C. Bocker<sup>3</sup>, D. Karashanova<sup>4</sup>,  
I. Mihailova<sup>1</sup>, I. Gugov<sup>1</sup>, C. Rüssel<sup>3</sup>

<sup>1</sup> University of Chemical Technology and Metallurgy, 8 Kl. Ohridski Blvd., 1756 Sofia, Bulgaria

<sup>2</sup> Institute of Physical Chemistry, Bulgarian Academy of Sciences, Acad. G. Bonchev Str, Block 11, 1113 Sofia, Bulgaria

<sup>3</sup> Otto Schott Institute for Materials Research, Jena University, Fraunhoferstr. 6, 07743 Jena, Germany

<sup>4</sup> Institute of Optical Materials and Technologies Bulgarian Academy of Sciences, Acad. G. Bonchev Str., Block 109, 1113 Sofia, Bulgaria

Received October, 2016; Revised December, 2016

The present work reports on the synthesis of BaTiO<sub>3</sub> containing glass-ceramics by applying appropriate annealing programs and varying the ratio of Na<sub>2</sub>O to Al<sub>2</sub>O<sub>3</sub> in a sodium-aluminoborosilicate glass. The phase composition is studied by X-ray diffraction and additionally to the presence of BaTiO<sub>3</sub>, also some silicate-based phases are detected. The microstructures of the obtained glass-ceramics are investigated by electron microscopy and depending on the ratio between Na<sub>2</sub>O and Al<sub>2</sub>O<sub>3</sub>, the presence of morphologically differing crystalline structures is concluded. Computed tomography is utilized to determine the volume fractions and size distributions of the barium titanate crystals in the glass ceramics. A high volume concentration of crystals is observed.

**Keywords:** barium titanate; crystallization; microstructure.

### INTRODUCTION

The efficient energy storage and energy consumption are some of the most acute and important problems nowadays. Thus, the synthesis and the investigation of the microstructure with respect to the physical properties of materials are of great importance. Barium titanate, BaTiO<sub>3</sub>, is a phase from the perovskite family – well-known since a long time – and with outstanding dielectric, pyroelectric, piezoelectric and even optical properties, as well as easy to prepare in the form of glass-ceramics. Barium titanate occurs in several crystallographic modifications (tetragonal, cubic, orthorhombic, rhombohedral and hexagonal) but two of them are especially interesting with respect to particular applications: the tetragonal which is ferroelectric and stable at room temperature and the cubic which is stable above the Curie temperature of approximately 120 °C and possesses paraelectric proper-

ties. Both phases have found applications in the preparation of different electronic devices, i.e. as powerful capacitors, as a substitute of the magnetic RAM, e.g. as FRAM [1–5]; multilayered capacitors for energy storage; capacitors for use in high power transmitters and microwave resonant cavities; piezoelectric elements and resistive sensors [1, 3, 4–6]. Depending on its optical properties, BaTiO<sub>3</sub> could be a promising candidate for laser preparation for optoelectronic applications [5]. Different experimental techniques are used to obtain barium titanate as bulk material, [1, 2, 4, 5]. The preparation of BaTiO<sub>3</sub> in the form of thin films and as separate crystalline beads which are subsequently calcined in larger aggregates is also reported in the literature [3, 6–8]. The stability of each barium titanate modification at room temperature is determined by the size, as well as by the used preparation technique and also by the addition of dopants [1, 2, 4, 6, 10]. Decisive for the controlled crystallization and size-distribution of the obtained crystals is mainly the preparation technique. Actually, there are a large number of methods to prepare barium titanate with or without dopants. Conventionally, barium titanate ceramics are prepared by the chemical reaction of

\* To whom all correspondence should be sent:  
E-mail: ruza\_harizanova@yahoo.com

barium carbonate and titanium oxide to barium titanate, accompanied by subsequent milling and sintering. [2]. Furthermore, the preparation of barium titanate nanorods, with potential applications in the construction of UV lasers, by means of a hydrothermal method is reported in Ref. [5]. Gelation and subsequent calcinations is reported in Ref. [7], in order to prepare beads of different perovskite crystals which are first obtained as cubic polymorph and then, after additional thermal treatment, the tetragonal modification is stabilized at room temperature. Also, the addition of appropriate dopants can lead – after applying a suitable time-temperature heat treatment – to composite crystals consisting of one ferroelectric and one ferromagnetic component, exhibiting multiferroic properties [9, 10]. The system  $(24-y)\text{Na}_2\text{O}/y\text{Al}_2\text{O}_3/14\text{B}_2\text{O}_3/37\text{SiO}_2/25\text{Fe}_2\text{O}_3$  with  $y = 8, 12, 14$  and  $16$  and other similar compositions were studied [11–14]. It was shown that in the obtained glasses initially phase separation occurs and droplets with sizes in the range from 100 to 800 nm enriched in  $\text{B}_2\text{O}_3$  and  $\text{FeO}_x$  are formed. Within these droplets, magnetite crystals with sizes in the range from 25 to 40 nm with potential application as multicore nanoparticles are precipitated [14].

The present paper reports on the synthesis, as well as on the phase and microstructural characterization of glasses and glass-ceramics with the composition  $23.1\text{Na}_2\text{O}/23.1\text{BaO}/23\text{TiO}_2/17.4\text{SiO}_2/7.6\text{B}_2\text{O}_3/5.8\text{Al}_2\text{O}_3$ , as well as the composition series  $(23.1-x)\text{Na}_2\text{O}/23.1\text{BaO}/23\text{TiO}_2/9.8\text{B}_2\text{O}_3/21\text{SiO}_2/x\text{Al}_2\text{O}_3$ ,  $x = 3, 7, 11$  mol%. The thermal treatment of the reported glasses results in the precipitation of barium titanate and various crystalline silicate phases. For samples in which only one crystalline phase occurs, morphology and size are investigated by scanning electron microscopy and computed tomography. The crystallization of large volume fractions of barium titanate crystals with crystallite sizes in the submicron and micrometer range is established. The occurrence of phase separation into Ba and Ti rich regions and subsequent crystallization of barium titanate in these regions is suggested.

## EXPERIMENTAL

Samples with mol% batch compositions  $23.1\text{Na}_2\text{O}/23.1\text{BaO}/23\text{TiO}_2/17.4\text{SiO}_2/7.6\text{B}_2\text{O}_3/5.8\text{Al}_2\text{O}_3$  (further denoted as composition A) and  $(23.1-x)\text{Na}_2\text{O}/23.1\text{BaO}/23\text{TiO}_2/9.8\text{B}_2\text{O}_3/21\text{SiO}_2/x\text{Al}_2\text{O}_3$ ,  $x = 3, 7, 11$  mol% (denoted as compositions B1, B2 and B3, respectively) were melted from the following reagent grade raw materials:  $\text{Na}_2\text{CO}_3$ ,  $\text{BaCO}_3$ ,  $\text{TiO}_2$ ,  $\text{Al}(\text{OH})_3$ ,  $\text{B}(\text{OH})_3$  and  $\text{SiO}_2$ . The glasses are melted in 60g batches for 1 h at 1400 °C in air using a Pt crucible in a furnace with  $\text{MoSi}_2$  heating elements.

The melts are quenched on a copper block without pressing. Then, in order to increase the mechanical stability and to minimize internal stresses, the glass was transferred to a pre-heated graphite-mould and held for 15 min at 480 °C in a muffle furnace. Subsequently, the furnace was switched off and the sample was allowed to cool to room temperature. Crystallization of the samples was, according to the DTA data, carried out at different temperatures and for different times in a muffle furnace as described in Ref. [15].

The phase compositions of the samples from all melted compositions are studied by X-ray diffraction (XRD), *Philips PW1050* using  $\text{Cu-K}\alpha$  radiation ( $\lambda = 1.5406 \text{ \AA}$ ) and Ni filter. The microstructure and the elemental composition of the prepared glasses and of the crystallized samples is further analysed by scanning electron microscopy (SEM) in combination with energy-dispersive (EDX) analysis, (*JSM-7001F*, *JEOL Ltd., Japan*) and (*Philips 515 with SEI detector*). Imaging of the crystallized samples is performed on polished samples or on fractured surfaces, or if this did not result in a good contrast, on samples etched for 5 s in 1% HCl solution. The average crystal size and volume fraction of selected samples was investigated by computed tomography (*x-ray microtomograph Brucker SkyScan 1272*).

## RESULTS AND DISCUSSION

The samples from the two sets of compositions A and B1-B3 freeze like glasses after pouring the melt, although for the samples A and B1 also some surface crystallization during cooling of the melt occurs – as already shown in [16]. Increasing alumina concentration at the expense of sodium oxide results in better glass formation and hence, surface crystallization does no longer occur in the compositions B2 and B3. This is attributed to the intermediate character of aluminium ions,  $\text{Al}^{3+}$  in the glass network and has widely been discussed in literature [12, 17–22] as well as in our previous work on similar compositions [14, 15, 23].

The compositions A and B1-B3 are annealed supplying different time-temperature schedules, according to the DTA data as reported in Refs. [15, 16]. Most samples annealed above  $T_g$  are visually crystalline even after 15 min annealing time and this is supported by the respective XRD patterns of the bulk specimens as shown in Figures 1a–d. All samples from Figs. 1a–d are annealed at the DTA crystallization peak maximum or near the respective temperature. The samples from composition A show only XRD peaks attributed to  $\text{BaTiO}_3$  (JCPDS 90-10-801). Applying longer annealing times results in a higher amount of the crystalline phase as expected

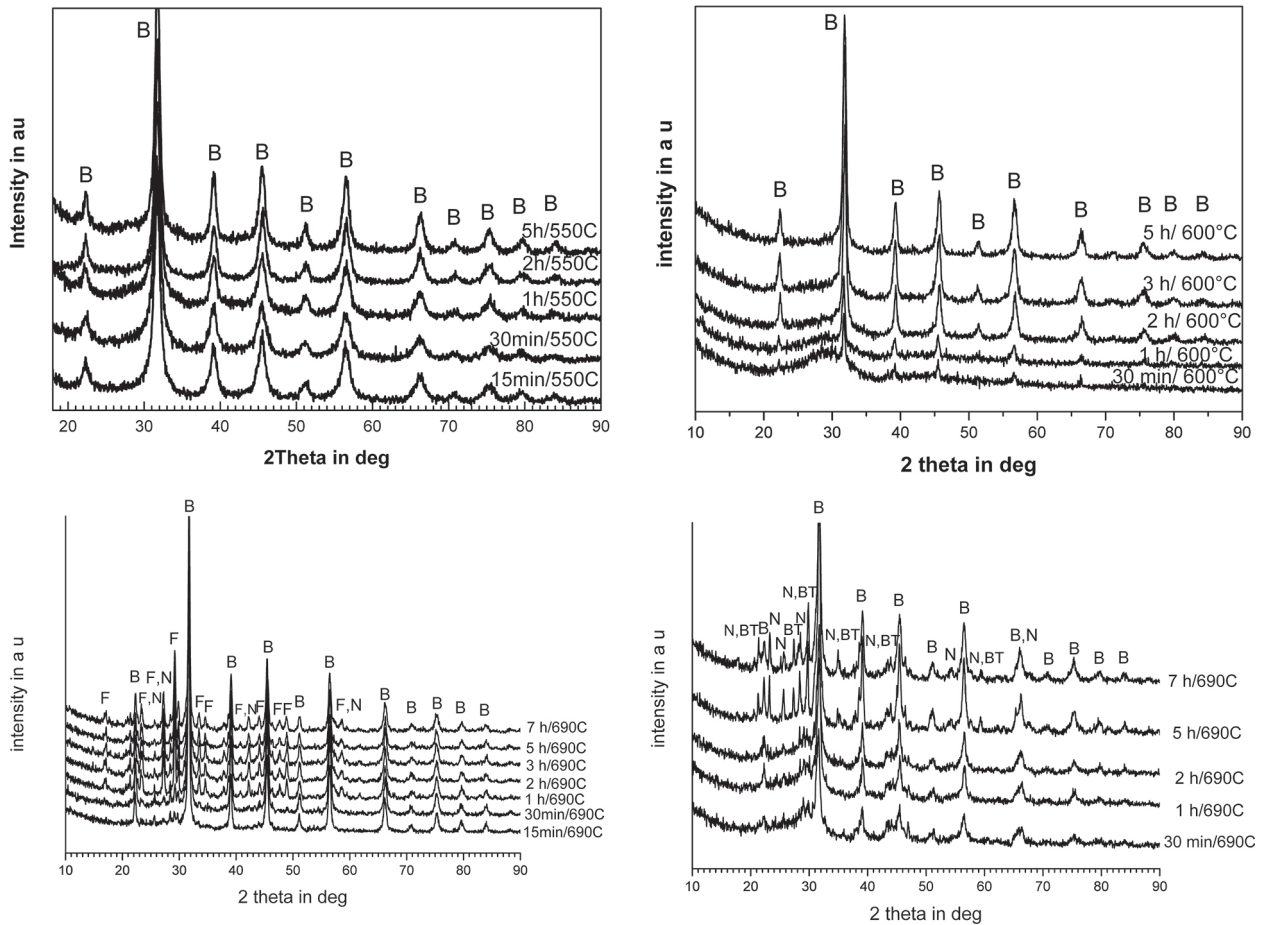


**Fig. 1.** a) XRD-patterns of samples with the composition A, annealed at the crystallization peak maximum in the DTA profile at 550 °C for different periods of time – cubic BaTiO<sub>3</sub> (B) formed; b) XRD-patterns of samples with the composition B1 – crystallization of cubic BaTiO<sub>3</sub> (B) after different periods of time at 600 °C; c) XRD-patterns of samples with the composition B2 annealed at 690 °C for different times – growth of cubic BaTiO<sub>3</sub> (B), Ba<sub>2</sub>TiSi<sub>2</sub>O<sub>8</sub> (F) and NaAlSiO<sub>4</sub> (N); d) XRD-patterns of samples with the composition B3 annealed at 690 °C for different times – growth of cubic BaTiO<sub>3</sub> (B), BaTi<sub>2</sub>O<sub>5</sub> (BT) and NaAlSiO<sub>4</sub> (N).

in the case of non-constraint isothermal crystallization. If samples B1 are thermally treated near the temperature of the crystallization peak maximum, e.g. the XRD patterns shown in Fig. 1b, the only crystalline phase formed is BaTiO<sub>3</sub>. However, the variation of the annealing temperature and more precisely, its increase, results for the samples with 3 mol% alumina (composition B1) in the formation of a second crystalline phase – Fresnoite, Ba<sub>2</sub>TiSi<sub>2</sub>O<sub>8</sub> (JCPDS 98-20-1844) as already observed in Ref. [16]. In contrast to the crystallization behaviour of samples with up to 6 mol% Al<sub>2</sub>O<sub>3</sub>, the XRD patterns of the crystallized specimens with 7 and 11 mol%, (compositions B2 and B3, respectively) are characterized by the occurrence of at least three crystalline phases namely Fresnoite and Nepheline, NaAlSiO<sub>4</sub> (JCPDS 35-0424) for B2 and Nepheline, NaAlSiO<sub>4</sub> and barium titanium oxide, BaTi<sub>2</sub>O<sub>5</sub> (JCPDS 70-1188) for B3, cf. Figs. 1c and 1d. Such

crystallization behaviour is supposed to be due to the increasing alumina concentration and the higher annealing temperatures which facilitate the nucleation and growth of Na- and Al-containing silicates [12]. Again, longer annealing times results in a larger crystals for one and the same annealing temperature. Actually, in Figs. 1c and 1d, it is seen that BaTiO<sub>3</sub> always occurs as the first crystalline phase precipitated which is attributed to the extremely high concentrations of Ba and Ti. However, for longer annealing times, the amount of the second precipitated phase, Nepheline also increases – especially well seen in Fig. 1d. The easier nucleation and growth of barium titanate, could be attributed to the occurrence of phase separation processes, as observed for similar systems [12, 16, 23, 24], into a Ba, Ti- rich phase and a matrix enriched in all other elements from the composition. Thus, the nucleation of BaTiO<sub>3</sub> starts first and after that for

example, nepheline despite the larger ionic radii of  $\text{Ba}^{2+}$  (1.35 Å) and  $\text{Ti}^{4+}$  ions (0.56 Å in tetrahedral and 0.75 Å in octahedral coordination) in comparison to those of  $\text{Na}^+$  (1.02 Å),  $\text{Al}^{3+}$  (0.54 Å) and  $\text{Si}^{4+}$  (0.40 Å). The  $\text{BaTiO}_3$  phase is recognized as the cubic modification because there is no visible splitting in the characteristic peak at about  $45.3^\circ$  – as it should be in the case for tetragonal  $\text{BaTiO}_3$  [1, 23–25]. Many authors report different symmetries of the  $\text{BaTiO}_3$  crystals depending on their size; the larger crystallites are normally tetragonal, while the smaller ones are cubic [1, 25] or a combination of a tetragonal core and a cubic shell is observed during the course of crystal growth [1]. Surprisingly, in the investigation of all the compositions A and B1-B3, despite the different annealing regimes and crystallite sizes, always cubic barium titanate is formed.

The microstructure of the synthesized glasses and the glass-ceramics obtained after thermal treatment was studied by scanning electron microscopy. The micrograph of sample A showed that the crystals formed at the surface are spherically shaped with dendritic needle-like structures as shown in Fig. 2. The shape of the crystallized regions suggests that probably phase separation occurs at some stages during cooling the melt and the spherical particles are enriched in the heavy elements, Ba and Ti which facilitates the formation of  $\text{BaTiO}_3$  crystals. The same behaviour has been observed for other similar glass systems and compositions as reported in Refs. [12–16, 24]. From Fig. 3, where sample A crystallized for 2 h at  $550^\circ\text{C}$  is shown, the precipitation of

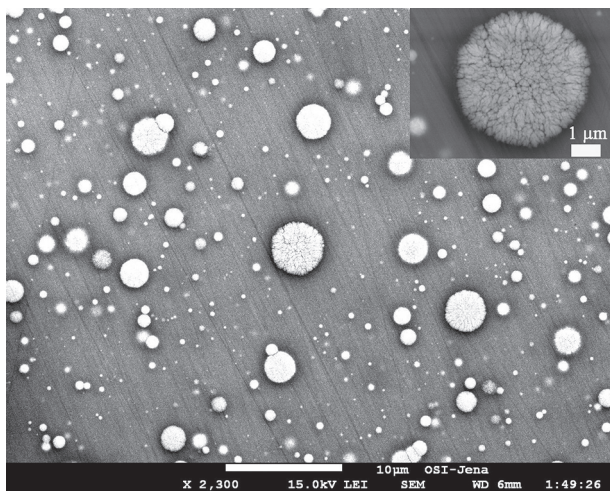


**Fig. 2.** SEM-micrograph of a sample with the composition A – glass without heat-treatment with crystals formed on the surface during pouring the melt. Inset: magnified SEM-micrograph of the glass A showing the morphology of the crystals formed at the surface.

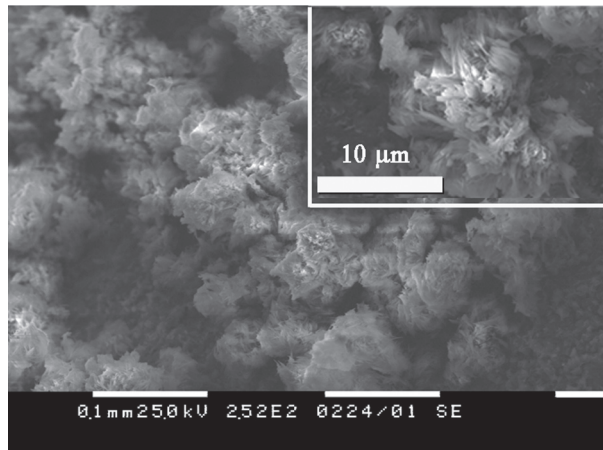


**Fig. 3.** SEM image of a sample A annealed for 2 h at  $550^\circ\text{C}$  – fractured surface showing growth of globular regions of needle-like crystals of  $\text{BaTiO}_3$ . The inset: magnified image of the same glass-ceramic sample revealing the morphology of the crystals.

a large volume fraction of  $\text{BaTiO}_3$  crystals gathered in spherically shaped agglomerates is seen. The latter possess sizes of up to hundred micrometers and consist of separate crystals growing together. The inset in Fig. 3 shows that between the spherical particles there are dark regions – the amorphous matrix where separate crystals are found. The morphology of the crystals corresponds to that of the crystals at the surface of sample A (Fig. 2). The SEM investigations of samples B1-B3 reveal that the increasing alumina concentration and the decreasing  $\text{Na}_2\text{O}$  concentration lead to a reduced tendency towards surface crystallization but to the same morphology of the growing crystals. Thermal treatment of sample B1 results in glass-ceramics with  $\text{BaTiO}_3$  as the only or at least as the dominating crystalline phase, as supported by the XRD patterns shown in Fig. 1b and from previous investigations reported in Ref. [16]. Here, the crystallization temperature of  $650^\circ\text{C}$  and annealing time 3 h lead to barium titanate crystals with similar shape to that in Fig. 3 and large volume fraction, as already reported in Ref. [16]. The results from the SEM imaging in Ref. [16] led to further microstructural investigations of sample B1 with the same thermal history (annealed 3 h at  $650^\circ\text{C}$ ) by means of computed tomography (see Fig. 4). The bright phase corresponds to the barium titanate crystals and the dark one – to the amorphous matrix and eventually to some Fresnoite crystals which possess a lower average atomic number, as witnessed by SEM in Ref. [16]. The image from Fig. 4 shows again crystals growing as spherically shaped agglomerates with an average size as determined from the processing of the image of around  $17\pm 3$  micrometers and a volume fraction of

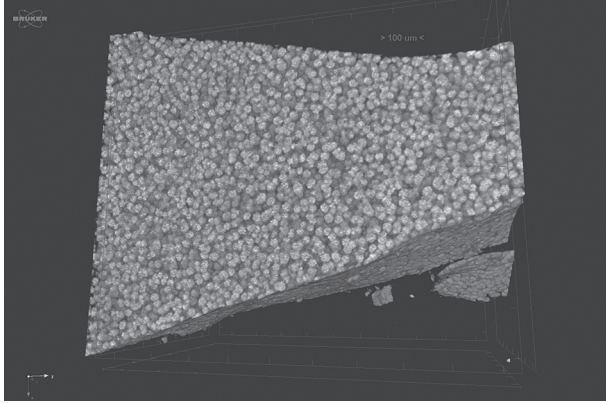


**Fig. 4.** Glass-ceramic B1 annealed 3h at 650 °C – imaging by means of computed tomography.

approximately  $58 \pm 1\%$ . The separate particles tend to aggregate and form larger complexes which grow together – as seen in Figures 2 and 3. Similar structures were already observed in other systems where the crystallization is preceded by droplet-like phase separation [14–16, 23, 24]. The microstructural investigation of all annealed samples B1 shows growth of only one morphological type of  $\text{BaTiO}_3$  crystals. Actually, the SEM investigations of samples with different thermal history and composition suggests that after annealing times  $t \geq 3$  h, the mean size of the formed globular crystals continues to grow and the separate spherical particles tend to form aggregates. This behaviour differs from the tendency described in [16, 23], where after thermal treatment for more than 3 h, the crystallite size stops increasing. The bright appearance of the formed crystals suggests that they contain the heavier elements of the initial composition, e. g. Ba and Ti. The addition of transition metal oxides other than Ti as dopants, for example Fe was studied in other composition series and is a well-known method for affecting the phase formation and thus, the properties of the resulting crystals [2–4, 8–10, 24, 25]. In Ref. [24], a composition similar to B1 is developed and its crystallization behaviour is reported. There, the presence of Fe leads additionally to the  $\text{BaTiO}_3$  crystallization also to that of  $\text{BaTi}_{0.75}\text{Fe}_{0.25}\text{O}_{2.888}$  which has a hexagonal symmetry and may possess multiferroic properties, as discussed in [2, 24].

The SEM-micrographs of the annealed samples B2 are characterized by the presence of more than one morphological type of crystals which is shown in Figure 5 for a sample annealed for 7 h at 690 °C. This supports the results from the XRD analyses of this composition shown in Fig. 1c.

Figure 6 shows an SEM micrograph of sample B3 annealed for 7 h at 690 °C where, as also wit-

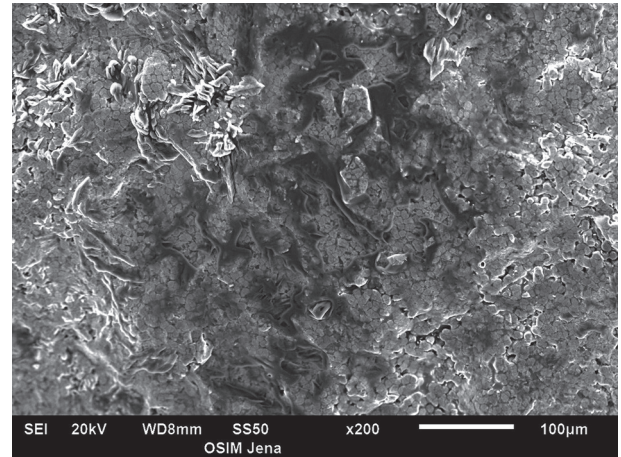


**Fig. 5.** SEM micrograph of a sample B2 crystallized for 7 h at 690 °C – at least two morphologically different types of crystals are present.

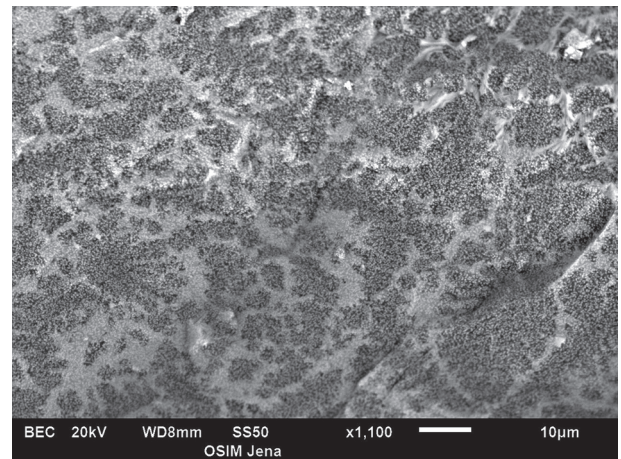


**Fig. 6.** SEM micrograph of a sample B3 crystallized for 7 h at 690 °C – presence of more than one morphological type of crystals.

nessed from the XRD patterns in Figure 1d, additionally to  $\text{BaTiO}_3$  other crystalline phases are present. The SEM micrographs shown in Figs. 5 and 6 reveal that the increasing alumina concentration and the decreasing sodium oxide concentration lead to smaller  $\text{BaTiO}_3$  crystals. This observation could be explained by the higher glass transition temperature and hence, the higher viscosity of the glass with the larger  $\text{Al}_2\text{O}_3$  concentration when crystallizing it at the same temperature (690 °C) as described in Ref. [15].

The observed phase composition and morphology of the formed crystals as well as the resulting size variation, depend on the composition of the initial glasses and will affect the dielectric properties

of the obtained glass-ceramic materials which will be a subject of further investigations.

## CONCLUSIONS

From melts with compositions 23.1Na<sub>2</sub>O/23.1BaO/23TiO<sub>2</sub>/7.6B<sub>2</sub>O<sub>3</sub>/17.4SiO<sub>2</sub>/5.8Al<sub>2</sub>O<sub>3</sub> and (23.1-x)Na<sub>2</sub>O/23.1BaO/23TiO<sub>2</sub>/9.8B<sub>2</sub>O<sub>3</sub>/21SiO<sub>2</sub>/xAl<sub>2</sub>O<sub>3</sub>, x = 3, 7 and 11 mol% glasses are obtained during cooling, although the larger sodium oxide concentrations in samples with 5.8 and 3 mol% alumina result in surface crystallization. The increasing alumina concentration leads to decreased crystallization tendency and smaller BaTiO<sub>3</sub> crystals for one and the same time-temperature schedule which is attributed to the increased viscosity of the glass. Small Al<sub>2</sub>O<sub>3</sub> concentrations and comparatively low crystallization temperatures result in the sole crystallization of BaTiO<sub>3</sub>, while at higher crystallization temperatures and times, a second crystalline phase, Fresnoite (Ba<sub>2</sub>TiSi<sub>2</sub>O<sub>8</sub>) is formed. The larger alumina concentrations, however, tend to facilitate the crystallization of two or more crystalline phases, at least one of them containing Al, i.e. Nepheline NaAlSi<sub>3</sub>O<sub>8</sub>. It is observed that BaTiO<sub>3</sub> always crystallizes as the first phase and the volume fraction of the crystals, as well as their average size for one and the same composition increases with increasing crystallization time. The method of the computed tomography is successfully utilized to estimate the average size of the barium titanate crystals to be about 17±3 micrometers and their volume fraction – of the order of 58±1% for the glass-ceramics with 3 mol% Al<sub>2</sub>O<sub>3</sub>.

**Acknowledgements:** This work was financially supported by means of contract NIS-11507, funded by UCTM.

## REFERENCES

1. J. F. Capsal, E. Dantras, L. Laffont, J. Dandurand, C. Lacabanne, *J. Non-Cryst Solids*, **356**, 629 (2010).
2. G. P. Du, Z. J. Hu, Q. F. Han, X. M. Qin, W. J. Shi, *J Alloys Compounds*, **492**, L79 (2010).
3. T. J. Jackson, I. Jones, *J Mater Sci*, **44**, 5288 (2009).
4. Z. Libor, S.A. Wilson, Q. Zhang, *J Mater Sci*, **46**, 5385 (2011).
5. R. Vijayalakshmi, V. Rajendran, *Digest J Nanomater Biostruc*, **5**, 511 (2010).
6. C. B. Carter, M. G. Norton, in: *Ceramic Materials: Science and Engineering*, 1<sup>st</sup> Ed., Springer, 2007.
7. A. F. Demirörs, A. Imhof, *Chem Mater*, **21**, 3002 (2009).
8. S. F. Mendes, C. M. Costa, C. Caparros, V. Sencadas, S. Lanceros-Mendez, *J Mater Sci*, **47**, 1378 (2012).
9. R. P. Maiti, S. Basu, S. Bhattacharya, D. Chakravorty, *J Non-Cryst Solids*, **355**, 2254 (2012).
10. H. T. Langhammer, T. Müller, T. Walther, R. Böttcher, D. Hesse, E. Pippel, S. G. Ebbinghaus, *J Mater Sci*, **51**, 10429 (2016).
11. R. Harizanova, G. Völksch, C. Rüssel, *J Mater Sci*, **45**, 1350 (2010).
12. W. Vogel, in: *Glasschemistry*, 3 Ed. Springer-Verlag, Berlin-New York-London-Paris-Tokyo-Hong Kong-Barcelona-Budapest, 1992.
13. R. Harizanova, I. Gugov, C. Rüssel, D. Tatchev, V. S. Raghuvanshi, A. Hoell, *J Mater Sci: Size Dependent Effects*, **46**, 7169 (2011).
14. C. Worsch, P. Schaaf, R. Harizanova, C. Rüssel, *J Mater Sci*, **47**, 5886 (2012).
15. R. Harizanova, L. Vladislavova, A. Mazhdrakova, C. Bocker, G. Avdeev, G. Tsutsumanova, I. Gugov, C. Rüssel, *Advances in Natural Science: Theory & Applications*, **3**, 21 (2014).
16. R. Harizanova, A. Mazhdrakova, L. Vladislavova, G. Avdeev, C. Bocker, I. Gugov, C. Rüssel, *J Chem Technol Metall*, **50**, 375 (2015).
17. K. El-Egili, *Phys B*, **325**, 340 (2003).
18. S. Hornschuh, B. Messerschmidt, T. Possner, U. Possner, C. Rüssel, *J Non-Cryst Solids*, **347**, 121 (2004).
19. L. Hong, P. Hrma, J. D. Vienna, M. Qian, Y. Su, D. E. Smith, *J Non-Cryst Solids*, **331**, 202 (2003).
20. D. Benne, C. Rüssel, M. Menzel, K. Becker, *J Non-Cryst Solids*, **337**, 232 (2004).
21. H. Schirmer, R. Keding, C. Rüssel, *J Non-Cryst Solids*, **336**, 37 (2004).
22. D. Benne, C. Rüssel, D. Niemer, M. Menzel, K. Becker, *J Non-Cryst Solids*, **345–346**, 203 (2004).
23. R. Harizanova, L. Vladislavova, C. Bocker, C. Rüssel, I. Gugov, *Bul Chem Comm*, **46**, 56 (2014).
24. R. Harizanova, M. Abrashev, I. Avramova, L. Vladislavova, C. Bocker, G. Tsutsumanova, G. Avdeev, C. Rüssel, *Solid State Sci*, **52**, 49 (2016).
25. S. D. Vacche, F. Oliveira, Y. Leterrier, V. Michaud, D. Damjanovic, J. E. Manson, *J Mater Sci*, **47**, 4763 (2012), DOI 10.1007/s10853-012-6362-x.

ИЗСЛЕДВАНЕ НА КРИСТАЛИЗАЦИОННОТО ПОВЕДЕНИЕ  
НА НАТРИЕВО-АЛУМОБОРОСИЛИКАТНИ СЪГЛА С ВИСОКА  
КОНЦЕНТРАЦИЯ НА БАРИЙ И ТИТАН

Р. Харизанова<sup>1\*</sup>, Д. Тачев<sup>2</sup>, Г. Авдеев<sup>2</sup>, Хр. Бокър<sup>3</sup>, Д. Карашанова<sup>4</sup>,  
И. Михайлова<sup>1</sup>, И. Гугов<sup>1</sup>, Хр. Рюсел<sup>3</sup>

<sup>1</sup> Химикотехнологичен и металургичен университет, бул. „Кл. Охридски“ № 8,  
1756 София, България

<sup>2</sup> Институт по физикохимия, БАН, ул. „Акад. Г. Бончев“, бл. 11, 1113 София, България

<sup>3</sup> Ото Шот институт за изследване на материалите, Университет Йена,  
ул. „Фраунхофер“ № 6, 07743 Йена, Германия

<sup>4</sup> Институт за оптични материали и технологии, БАН, ул. „Акад. Г. Бончев“,  
бл. 1091, 1113 София, България

Постъпила октомври, 2016 г.; приета декември, 2016 г.

(Резюме)

В настоящата работа е докладван синтезът на стъклокерамики, съдържащи бариев титанат,  $BaTiO_3$  в натриево-алумоборосиликатни стъкла чрез прилагане на подходящи термични програми за отгряване и чрез промяна в съотношението на концентрациите на  $Na_2O$  и  $Al_2O_3$ . Фазовият състав е изучен с използване метода на рентгеновата дифракция и допълнително на присъствието на  $BaTiO_3$ , е установена кристализацията на няколко силикатни фази. Микроструктурата на получените стъклокерамики е изследвана по метода на електронната микроскопия и в зависимост от съотношението в концентрациите на  $Na_2O$  и  $Al_2O_3$ , е установено наличието на различни като морфология кристални структури. Микрокомпютърната томография е използвана за определяне на обемното съдържание на кристалната фаза и разпределението по размери на бариєво-титанните кристали в стъклокерамиките. Установено е високо обемно съдържание на кристалната фаза.